

Review Article

## Excess Electrons in Polar Cluster Anions†

H. Abdoul-Carime, Y. Bouteiller, C. Desfrancois, L. Philippe and J. P. Schermann\*

Laboratoire de Physique des Lasers, Institut Galilée, Université Paris-Nord, 93430, Villetaneuse, France

Abdoul-Carime, H., Bouteiller, Y., Desfrancois, C., Philippe, L. and Schermann J.P., 1997. Excess Electrons in Polar Cluster Anions. – Acta Chem. Scand. 51: 145–150. © Acta Chemica Scandinavica 1997.

Different mechanisms are involved in thermal electron attachment to assemblies of closed-shell polar molecules. Dipole-bound anions can be created from small clusters with total resultant dipole moments that are larger than a critical value of 2.5 D. The cluster anion excess electrons are in very diffuse orbitals located outside the molecular frame. Anions and their neutral parents then have the same geometrical structures. The electron binding energies are very small and external electric fields can easily detach the excess electrons. Excess electrons can be localized in valence orbitals of closed-shell polar molecules with dipole moments smaller than 2.5 D if these molecules are imbedded in small non-homogeneous clusters. Solvation effects then lead to the formation of covalent anions. Excess electrons can also be collectively bound by large polar clusters and the corresponding anions are similar to solvated electrons in liquids.

The study of negatively charged clusters provides models for understanding the behaviour of excess electrons in condensed phases.<sup>1</sup> The different processes for anion formation in liquids are then investigated by considering electron attachment to solvated molecules in the thermal energy range. Negative ion formation is usually described as the accommodation of an excess electron in an unoccupied molecular orbital, corresponding to the production of ‘conventional’ or ‘covalent’ anions. Electron attachment to isolated polar, closed-shell molecules raises interesting questions since, individually, these molecules have high-lying LUMOs corresponding to negative electron affinities and thus should be unable to become parents of bound stable anions. However, in solution, these molecules can acquire positive electron affinities, due to solvation effects. Here we examine the modification of electron attachment properties of polar, closed-shell molecules, starting from isolated species in the gas-phase and progressively adding solvent molecules. Many solvents (e.g., water, ammonia, acetonitrile, pyridine) or biological molecules (e.g., DNA and RNA bases, amino acids) belong to this category and are commonly involved in oxidation–reduction processes.

The adiabatic electron affinity is a crucial thermodynamic parameter which governs anion production and it is defined as the energy difference between the neutral

parent and its daughter anion, both in their relaxed ground state. The observation of long-lived stable anions usually implies a positive value of this quantity. It has been demonstrated, either by quantum calculations<sup>2,3</sup> or free electron scattering experiments,<sup>4</sup> that isolated closed-shell molecules have negative electron affinities. Thus, when free electrons are scattered by closed-shell molecules, only ephemeral anions can appear as resonances with lifetimes lying in between  $10^{-12}$  and  $10^{-15}$  s. The existence of these resonances is due to the shape of the effective electron–molecule potential, which is the sum of a large distance attractive polarisation combined with the repulsive centrifugal term and a short-range potential. An excess electron is then temporarily trapped by the potential barrier. When the attaching molecules are polar, a totally different mechanism can take place for anion production. Owing to the long-range attractive dipole-field, under certain circumstances, which we will further examine, long-lived (with lifetimes exceeding microseconds) anions can then be experimentally observed with excess electrons nearly totally located *outside* the molecular frame. These anions, so called ‘dipole-bound anions’, retain the nuclear configuration of their neutral parents and the electron attachment process does not introduce any perturbation. Moreover, this ionisation process is *reversible* since the electron binding energy is so low that a weak electric field externally applied can detach the excess electron.

After studying electron attachment to isolated polar

† Lecture held at the 14th International Conference on Radical Ions, Uppsala, Sweden, July 1–5, 1996.

\* To whom correspondence should be addressed.

closed-shell molecules, in particular some molecules of biological interest, and the field-detachment reverse process we will consider the competition between ‘covalent’ binding and ‘dipole-binding’ for polar molecules with definite positive electron affinities. We will then examine the influence of solvation in polar clusters and the possibility of determination of small cluster anion structures. We will finally consider anion formation by collective electron binding in larger clusters.

### Dipole-binding to isolated polar molecules

An electron can be bound in a Coulomb  $-\beta/r$  potential in an infinite number of discrete states, whatever the  $\beta$  value. The behaviour of an electron in a dipolar potential  $-\mu/r^2$  is very different since bound discrete states exist only if  $\mu$  is larger than a critical value.<sup>5</sup> It was predicted in the early seventies that polar molecules with dipole moments larger than 2 D should bind electrons<sup>6</sup> but a systematic search for an experimental value of this critical dipole moment appeared only recently.<sup>7</sup> The theory of dipole-binding of electrons to polar molecules has been established by Clary.<sup>8</sup> The excess electron wavefunction can be obtained by means of the numerical resolution of the Schrödinger equation of an electron-polar molecule pseudopotential which is the sum of a dipolar  $-\mu \cos \theta/r^2$  term, a cut-off charge-induced dipole  $-(\alpha/r^4)(1-\exp[-(r/r_0)^6])$  term ( $r_0$  reflects the approximate size of the molecule and is taken to be  $\alpha^{1/3}$  where  $\alpha$  is the molecular polarizability) and a short-range repulsive term  $V_c \exp[-(r/r_c)^6]$ . An example of an iso-density electronic map is given in Fig. 1, which shows that the wavefunction is extremely diffuse and has an approximate hybrid  $sp_z$  character. This result has also been demonstrated by Adamowicz<sup>9</sup> using *ab-initio* calculations at the MP2 level. It is important to note that the dipole moment of the attaching molecule is not the only important parameter, but that the molecular polarizability must also be taken into account.

The weak binding energy  $E_A$  (between 0.1 and 100 meV) and the very diffuse character of the excess electron wavefunction in dipole-bound anions suggest rather strong similarities between these anions and atoms in very excited states (Rydberg atoms). For example, detachment of the excess electron is possible in both cases by means of small or moderate electric fields. For a  $-\mu/r^2$  potential, the critical detachment field  $F_c$  is related to the electron binding energy by  $E_A^3 = 27 \mu F_c^2 / 4$ . In practice, this relationship can fruitfully be used to determine directly such weak electron binding energies.<sup>10</sup> Dipole-binding is thus a unique ionisation process since it is reversible. Experimentally, it allows for an initial mass selection of anions followed by a recovery of the neutral parents without any internal excitation. For mass-spectrometry applications in gas-phase chemistry, it can be considered as the reverse technique of neutralization-reionisation mass spectrometry<sup>11</sup> where polyatomic

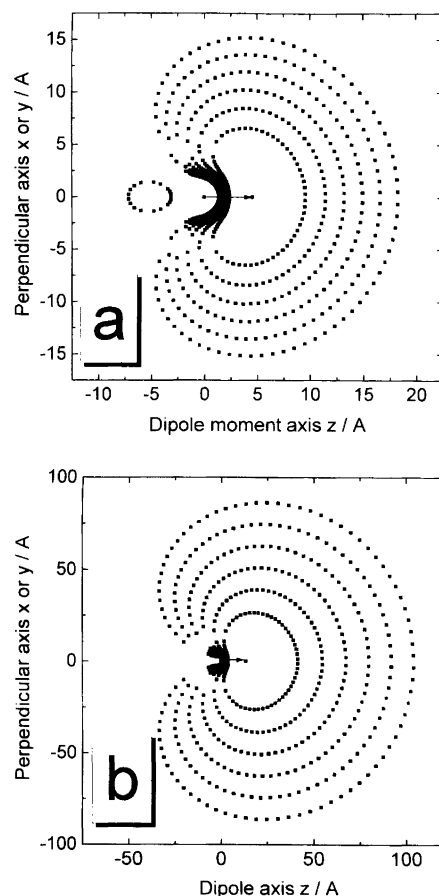


Fig. 1. Maps of the electron densities of dipole-bound anion excess electron orbitals. The arrows represent the molecular dipoles equal to 7 D (a) and 2.88 D (b). The successive dotted lines correspond to electron densities divided by a factor of three. The corresponding excess electron binding energies are, respectively, 176 meV and 3 meV.

organic intermediates are detected by first neutralising ions and further reionising them.

Dipole-bound anions can be produced by either free electron attachment<sup>12</sup> or charge-exchange collisions between Rydberg atoms and polar systems.<sup>13</sup> In each case, a third body is necessary in order to stabilise the nascent anions against the reverse process, i.e., electron autodetachment. Dipole-bound anions were first observed by Haberland and co-workers<sup>14</sup> who injected electrons in the high pressure region of a supersonic beam expansion. This technique provides large anion yields which allow for photodetachment studies leading to the determination of accurate vertical detachment energies.<sup>15</sup> However, the stabilization process is then due to collisions of the nascent anions with the supersonic expansion carrier gas and only anions with large enough binding energies (typically, several tens of millielectronvolts) can survive to collisional detachment. In charge transfer collisions with Rydberg atoms, a third body is already provided by the presence of the ionic positive core of the excited atom. The creation process is very selective with respect to the anion excess electron binding

energy. This can be understood if one considers<sup>10</sup> a Rydberg atom  $A^{**}(n)$ , with principal quantum number  $n$  and ionisation potential  $E_i(A) = \text{Ryd}/n$  (Ryd is the Rydberg constant). For simplicity, we neglect the Rydberg atom angular momentum  $l$ . This atom collides with a polar molecular system  $M$  with electron affinity  $E_A(M)$ . The covalent  $[A^{**}(n) + M]$  potential energy curve crosses the ionic  $[A^+ + M^-]$  curve at an atom-molecule internuclear distance  $R_c = 1/[E_i(A) - E_A(M)]$ . The electron exchange probability  $p$  at each potential energy curve crossing is a rapidly varying function of  $R_c$ . The overall charge-exchange probability  $P$  is proportional to the product  $p(1-p)$  and is thus maximum when  $p \approx 1/2$ . In order to produce a given dipole-bound anion  $M^-$ , for a given value of  $E_A(M)$ , we can consider two extreme cases. If the quantum number  $n$  of the Rydberg atom  $A^{**}(n)$  is too small, the crossing distance  $R_c$  is small, the overlap between the exchanged electron orbitals in the excited atom and in the anion is large,  $p$  is close to unity and the charge-exchange probability is negligible. The electron first transfers to the molecular system and immediately returns to the Rydberg atom orbital. If  $n$  is too large, the overlap is too weak and the electron transfer fails. There exist optimum values  $n_{\text{opt}}$  which correspond to maxima of the charge-transfer rates [Fig. 2(a)]. Experimentally, the following relationship between  $E_A(M)$  and  $n_{\text{opt}}$  has been observed:  $E_A(M) \approx 23 \text{ eV}/n_{\text{opt}}^{2.8}$  for a large number of anions created from electron attachment to polar molecules and clusters (Fig. 3).

The experimental signatures of dipole-bound anions are thus the following: (a) a strongly peaked  $n$ -dependence (around  $n = n_{\text{opt}}$ ) of the Rydberg electron transfer rates [Fig 2(a)], in contrast with the smooth  $n$ -dependences observed when covalent anions are produced,<sup>16</sup> (b) a steep and monotonic electric field detachment curve<sup>13</sup> [Fig 2(b)]; covalent anions have large electron binding energies and cannot be field-detached, (c) in the photoelectron spectra, single principal peaks at low vertical energy (VDE) are observed.<sup>15</sup> A large number of dipole-bound anions have been observed<sup>17</sup> with neutral parents possessing dipole moments lying between 2.5 and 4.5 D. Isolated molecules such as aldehydes, ketones and nitriles are the most common in this range, as well as their small clusters, together with elementary biological molecules, which are now considered.

### Electron attachment to nucleic acid bases

When ionising radiations interact with living cells, electrons are created which tend to localise on nucleic acid bases.<sup>18</sup> These DNA and RNA bases (as well as several amino acids) are strongly polar molecules and thus are candidates for dipole-binding of electrons,<sup>9</sup> at least when they are isolated in the gas phase. Under usual conditions, these molecules are strongly linked together by hydrogen bonds in microcrystals and are thus somewhat difficult to vaporise since chemical decomposition tends to occur

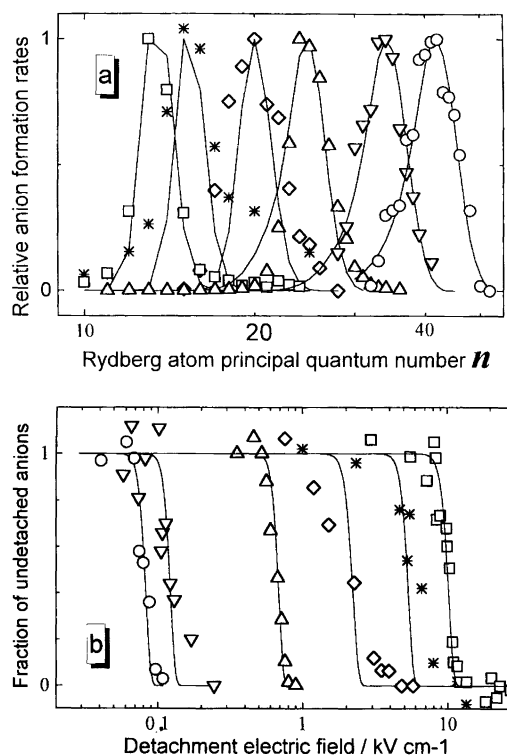


Fig. 2. (a) Experimental Rydberg electron transfer rates, as a function of the Rydberg atom principal quantum number  $n$ , for six dipole-bound anions ( $\circ$ , acetaldehyde;  $\nabla$ , butanal;  $\triangle$ , acetone;  $\diamond$ , methanol dimer;  $*$ , acetonitrile trimer;  $\square$ , water-ammonia dimer). These curves are peaked and their fitted curves (full curves) provide the following respective electron affinities: 0.7, 1.3, 3.0, 5, 11 and 15 meV. (b) Experimental field-detachment curves, as a function of an externally applied electric field, for the same dipole-bound anions as in (a). For each anion, the curve is independent of the Rydberg  $n$ -values.

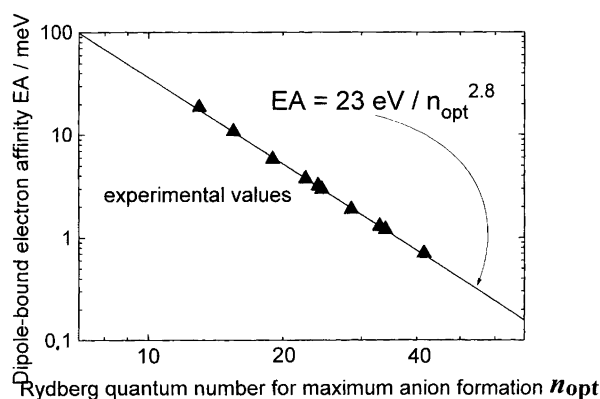


Fig. 3. The experimental values ( $\Delta$ ) of dipole-bound electron affinities  $E_A(M)$  are plotted (on a log-log scale) as a function of the Rydberg principal quantum numbers  $n_{\text{opt}}$  which leads to the maximum value of the electron transfer rates. The straight line corresponds to the  $E_A(M) \approx 23 \text{ eV}/n_{\text{opt}}^{2.8}$ .

before sublimation. Up to now, only dipole-bound anions of isolated adenine, thymine and uracyl have been studied either by Rydberg electron attachment<sup>19</sup> or photoelectron

spectroscopy.<sup>20</sup> Fig. 4 displays the  $n$ -dependences for the formation of anions in collisions between Rydberg atoms and adenine monomers or dimers. The adenine neutral monomer has a dipole moment equal to 2.4 D and a large polarisability ( $\text{\AA}^3$ ). The covalent electron affinity of this monomer is negative and equal to  $-0.3$  eV and the dipole-bound electron affinity is only 12 meV. The dimer has a positive covalent affinity. From a biological point of view, these dipole-bound anions are probably not relevant since water molecules are always present in a DNA double helix and electron attachment must be considered in the presence of this solvent.<sup>21</sup>

### Competition between dipole-binding and covalent binding

Some molecules, such as nitromethane or nitroethane, possess large dipole moments ( $\approx 3.5$  D) together with relatively large positive electron affinities ( $E_A \approx 0.2$ – $0.4$  eV). Thus, valence states (covalent anions) and dipole-bound states should coexist.<sup>22</sup> As shown in Fig. 5(a), the  $n$ -dependence of the formation rate of nitroethane anions produced in collisions with Rydberg  $\text{Xe}^{**}(n)$  atoms is peaked but much broader than usual for pure dipole-bound anion cases (see Fig. 2). Using the simple law given above, the maximum value  $n_{\text{opt}}=13$  leads to an estimate of the dipole-bound electron affinity  $E_{A_{\text{dip}}} \approx 15$  meV. Measurements of the electric field detachment properties of the anions formed by collisions with Rydberg atoms at different  $n$ -values provide clues for the interpretation of the electron attachment mechanisms. Fig. 5(b) displays two curves each corresponding to field detachment of  $\text{C}_2\text{H}_5\text{NO}_2^-$  anions created by collisions with Rydberg atoms with principal quantum numbers  $n=16$  and  $n=10$ . For  $n=16$ , all anions are field-detached if electric fields larger than  $15 \text{ kV cm}^{-1}$  are applied while, for  $n=10$ , only a small fraction of anions is detached, even for applied electric fields larger than  $30 \text{ keV cm}^{-1}$ . At large Rydberg  $n$ -values, electron exchange takes place at very large atomic ionic core–molecule internuclear

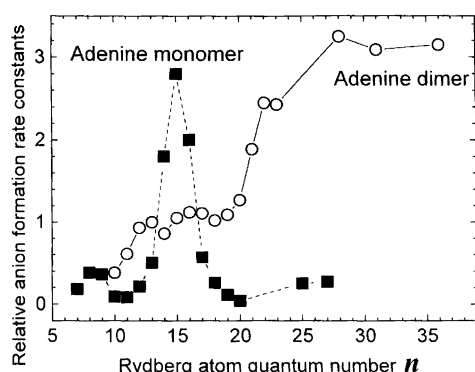


Fig. 4. Experimental  $n$ -dependences of the Rydberg electron transfer rates for production of adenine monomer and adenine dimer anions. The monomer curve corresponds to the formation of a pure dipole-bound anion and the dimer curve to a covalent anion.

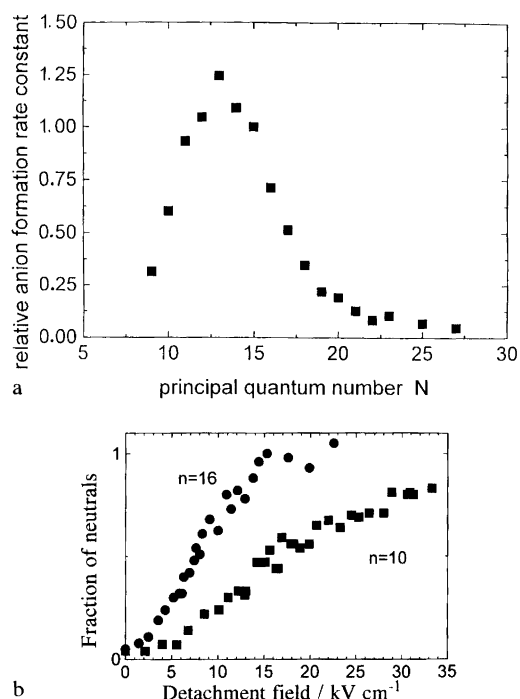


Fig. 5. (a) Experimental  $n$ -dependence of the Rydberg electron transfer rate for production of nitroethane anions. This curve is much wider than for pure dipole-bound anion formation [see Fig. 2(a)]. (b) Experimental field-detachment curves of nitroethane anions produced by electron transfer from Rydberg atoms with principal quantum number  $n=10$  or  $n=16$ . For  $n=16$ , the excess electrons are totally detached above  $15 \text{ kV cm}^{-1}$  and the anions are in a pure dipole-bound state. For  $n=10$ , anions have been partially vibrationally relaxed by the Rydberg ionic core and are in a superposition of dipole-bound and covalent states. They can no longer be totally field-detached.

distances and the amount of nascent anion internal energy is very small. The observed field-detachment behaviour then corresponds to production of dipole-bound  $\text{C}_2\text{H}_5\text{NO}_2^-$  anions which have the same linear equilibrium geometry as their neutral parent. At low  $n$ -values, the presence of the Rydberg ionic core at rather short distances induces a vibrational coupling between the dipole-bound state and the ground covalent state. It also takes away a sizeable fraction of the anion excess vibrational energy. The dipole-state, with an excess electron orbital that is diffuse and located on the ethyl group side, then appears as a metastable state which can be coupled to the covalent ground state if the molecule is distorted to the bent geometry. The excess electron orbital has then shifted towards the  $\text{NO}_2$  side in the covalent state.

### Homogeneous polar clusters. Determination of the geometrical structures

Dipole-binding of electrons can be a powerful means of ionisation. It allows for mass-selection of both negatively charged particles and neutral particles (following field-

detachment). van der Waals or hydrogen-bonded clusters can adopt a variety of geometries. The different isomer configurations are more or less populated according to the internal cluster temperature typically lying in the range 100–200 K. When the constituents are polar, each geometrical configuration corresponds to a resultant dipole moment which can be determined from Rydberg electron attachment measurements and structure calculations. The set of geometrical configurations can be determined by a detailed exploration of the multidimensional potential energy surfaces of the clusters.<sup>23</sup> Let us consider the example of acetonitrile clusters. The acetonitrile monomer possesses a large dipole moment of 3.92 D and  $\text{CH}_3\text{CN}^-$  anions are observed by means of Rydberg electron attachment around  $n_{\text{opt}} = 13$ . No  $(\text{CH}_3\text{CN})_2^-$  are observed since the lowest energy configuration of the neutral dimer is antiparallel with zero dipole moment. The lowest energy configurations of the neutral trimer possess dipole moments in the range 3.5–3.8 D while those of the tetramer consist of two antiparallel pairs with zero dipole moments. When the cluster size increases, the number of configurations increases rapidly. For  $(\text{CH}_3\text{CN})_5$ , several low energy configurations are populated with dipole moments between 2.1 and 3.9 D. As shown in Fig. 6, the Rydberg  $n$ -dependences for the creation of acetonitrile anions with a small odd number of molecules are characteristic of dipole-bound anions. Knowledge of the structure of the neutral parents provides the necessary information to predict the existence and the properties of the corresponding radical ions.

### Non-homogeneous polar clusters. Influence of solvation upon electron attachment

The presence of a solvent strongly influences the ability of molecules to bind electrons. A large number of molecules that possess negative electron affinities when

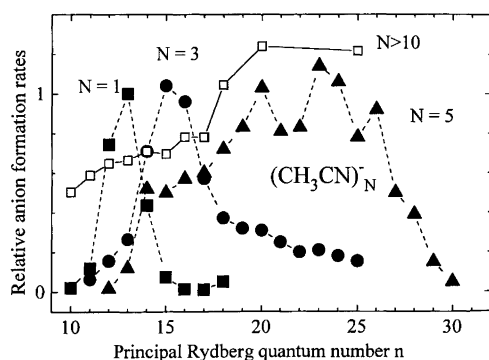


Fig. 6. Experimental  $n$ -dependences of the Rydberg electron transfer rates for production of acetonitrile anions. The monomer ( $\blacksquare$ ) and the trimer ( $\bullet$ ) curves are characteristic of pure dipole-bound anions with a single geometrical configuration. The different peaks of the pentamer curve ( $\blacktriangle$ ) correspond to different isomer configurations (see the text). The curve for production of  $(\text{CH}_3\text{CN})_{N>10}^-$  anions ( $\square$ ) is characteristic of covalent anions interpreted to be solvated electrons (see the text).

they are isolated in the gas-phase have positive affinities in the liquid phase. For example, water or ammonia are closed-shell polar molecules with highly negative electron affinities ( $\approx -8$  eV) and solvated electrons are observed in liquids.<sup>24</sup> In order to investigate the solvation effects, let us first consider non-homogeneous clusters formed by a closed-shell molecule  $M$  surrounded by  $N$  solvent molecules  $S$ . The absolute value of the negative electron affinity  $E_A(M)$  of  $M$  is smaller than the negative electron affinity of  $S$  and thus an excess electron in an  $(M \dots S_N)^-$  anion will be mostly localised on the 'electron chromophore'  $M$ . The electron affinity  $E_A(M, N)$  of the  $M \dots S_N$  cluster is related to  $E_A(M)$  by the following relationship:<sup>26</sup>

$$E_A(M, N) = E_A(M) + E_{\text{sol}}^N - D_0(M \dots S_N)$$

$E_{\text{sol}}^N$  is the solvation energy of the  $M^-$  ion surrounded by  $N$  solvent molecules.  $D_0(M \dots S_N)$  is the energy of the most stable configuration of the neutral  $M \dots S_N$  cluster. Since attractive negative charge–dipole interactions of an anion with its surroundings are stronger than neutral–neutral interactions, each added solvent molecule increases the adiabatic electron affinity by an amount  $\Delta E$  in the range 100–300 meV. To a first approximation, we can assume that  $\Delta E$  is nearly constant in a given system and thus  $E_A(M, N) \approx E_A(M) + N\Delta E$ . The adiabatic electron affinity of the cluster becomes positive above a size threshold  $N_{\text{th}}$  given approximately by  $N_{\text{th}} = -E_A(M)/\Delta E$ . Examples of size thresholds  $N_{\text{th}}$  corresponding to the observation of covalent anions are given Table 1. In these solvated anions, we have formulated the hypothesis that the excess electron charge is localised on a single molecule. The influence of a solvent molecule is sizeable only in the first solvation layer.<sup>26</sup> The solvation contribution of any molecule added in the second or larger solvation shell becomes very small since the distance between it and the localised charge is too large and the first solvation shell plays a screening role. It is then necessary to invoke a different mechanism to explain the existence of anions if the size threshold for observation of covalent anions from polar closed-shell clusters becomes larger than 10 molecules.

Table 1. Experimental number  $N_{\text{th}}$  of solvent molecules required for observation of covalent anions by electron attachment to a polar closed-shell molecule  $M$  with electron affinity  $E_A(M)$ .

Solvated molecule $M$	Electron affinity $E_A(M)/\text{eV}$	Solvent molecule	$N_{\text{th}}$
Acrylonitrile	−0.2	Acrylonitrile	2
Pyridine	−0.45	Pyridine	4
Chlorobenzene	−0.6	Chlorobenzene	4
Acetone	−1.15	Acetone	5
Phenol	−1.0	Water	6
Pyridine	−0.45	Water	3
Pyridine	−0.45	Phenol	1

## Solvated electrons

The binding of electrons to clusters of polar closed-shell molecules with large absolute values  $|E_A(M)|$  of their negative electron affinities is still a challenging problem. Molecules such as water or ammonia are isoelectronic with neon and their dipole moments are well below the critical value of 2.5 D for dipole-binding of electrons. For water, the mass distribution of  $(H_2O)_N^-$  anions below  $N=11$  are not regular, but rather 'magic'. The most abundant anions correspond to  $N=2,6$  and 7. Small ammonia clusters anions do not exist. It has been shown by several experiments<sup>27</sup> that smooth  $(H_2O)_N^-$  and  $(NH_3)_N^-$  anion mass distributions exist above respective size thresholds  $N_{th}=11$  for water and  $N_{th}=34$  for ammonia. The Rydberg  $n$ -dependences<sup>28</sup> and the photoelectron mass spectra<sup>29</sup> are characteristic of the production of covalent anions. As shown in Fig. 6, the Rydberg  $n$ -dependence of the rate constant for creation of  $(CH_3CN)_{N>10}^-$  anions is not peaked like for small anions but rather smooth, indicating that these large anions are covalent anions. These large anions cannot be field-detached. When cluster sizes become very large, electron binding energies tend towards the liquid bulk values.<sup>15,29</sup> The dipole configurations responsible for the observation of magic behaviour for small size are no longer important. Several quantum calculations have been developed to interpret the existence of these large water and ammonia clusters anions.<sup>29,30</sup> It has been shown that excess electrons may be initially trapped by local high dipole configurations at the cluster surface ('surface states') and that a further rearrangement of the cluster dipoles takes place, which strongly localises the excess electron ('interior states'). However, none of these models has been able, up to now, to predict correctly the size thresholds.

## Conclusions

Electron attachment to assemblies of closed-shell polar molecules leads to a rich variety of anions. The transition from the properties of isolated molecules to those of small molecular assemblies becomes reasonably well understood. Excess electrons in these cluster anions can be totally outside the molecular frames in very diffuse orbitals, well localised in a valence orbital of a single molecule or delocalized over the interior of whole large cluster. These studies have been conducted in the gas-phase and may help for the understanding of phenomena in condensed phases. However, comprehension of the gradual transition from the properties of medium-sized clusters to those of infinite bulk or biological systems will still require much experimental and theoretical work.

## References

1. Illenberger, E. *Chem. Rev.* 92 (1992) 1589.
2. Younkin, J. M., Smith, L. J. and Compton, R. N. *Theor. Chim. Acta* 41 (1976) 157.

3. Simons, J. and Jordan, K. D. *Chem. Rev.* 87 (1987) 535.
4. Nenner, I. and Schulz, G. J. *J. Chem. Phys.* 62 (1975) 1747.
5. Fermi, E. and Teller, E. *Phys. Rev.* 72 (1947) 406.
6. Garrett, W. R. *Phys. Rev.* 153 (1971) 961.
7. Desfrancois, C., Abdoul-Carime, H., Khelifa, N. and Schermann, J. P. *Phys. Rev. Lett.* 73 (1994) 2436.
8. Clary, D. C. *J. Phys. Chem.* 92 (1988) 3173.
9. Oyler, N. and Adamowicz, L. *J. Phys. Chem.* 97 (1993) 11122; Oyler, N. and Adamowicz, L. *Chem. Phys. Lett.* 219 (1994) 223.
10. Desfrancois, C. *Phys. Rev. A* 51 (1995) 3667.
11. Goldberg, N. and Schwartz, H. *Acc. Chem. Res.* 27 (1994) 347.
12. Arnold, S. T., Eaton, J. G., Patel-Mistra, D., Sarkas, H. S. and Bowen, K. H. In: Maier, J. P., Ed., *Ion and Cluster Ion Spectroscopy and Structure*, Elsevier.
13. Desfrancois, C., Baillon, B., Schermann, J. P., Arnold, S. T., Hendricks, J. H. and Bowen, K. H. *Phys. Rev. Lett.* 72 (1994) 48.
14. Haberland, H., Schindler, H. G. and Worsnop, H. G. *Ber. Bunsenges. Phys. Chem.* 88 (1984) 270; Haberland, H., Ludewigt, H., Schindler, C. and Worsnop, D. R. *Phys. Rev. A* 36 (1987) 967; Coe, J. V., Lee, G. H., Eaton, J. G., Arnold, S. T., Sarkas, H. W., Bowen, K. H., Ludewigt, C., Haberland, H. and Worsnop, D. R. *J. Chem. Phys.* 92 (1990) 3980.
15. Hendricks, J. H., de Clercq, H. L., Lyapustina, S. A., Francher, C. A., Lippa, T. P., Collins, J. M., Arnold, S. T., Lee, G. H. and Bowen, K. H. *Structures and Dynamics of Clusters (Yamada Conference XLIII Proc.)*, Universal Academy Press, Tokyo 1996.
16. Harth, K., Ruf, M.-W. and Hotop, H. *Z. Phys. D* 14 (1989) 149; Kraft, T., Ruf, M.-W. and Hotop, H. *Z. Phys. D* 14 (1989) 179.
17. Desfrancois, C., Abdoul-Carime, H. and Schermann, J. P. *Int. J. Mod. Phys. B* 10 (1996). *In press.*
18. Steenken, S. *Chem. Rev.* 89 (1989) 503.
19. Desfrancois, C., Abdoul-Carime, H. and Schermann, J. P. *J. Chem. Phys.* 104 (1996) 7792.
20. Hendricks, J., Lyapustina, S. A., de Clercq, H. L., Snodgrass, J. T. and Bowen, K. H. *J. Chem. Phys.* 104 (1996) 7788.
21. Colson, A. O. and Sevilla, M. D. *Int. J. Radiat. Biol.* 67 (1995) 627; Sevilla, M. D., Besler, B. B. and Colson, A. O. *J. Phys. Chem.* 99 (1995) 1060.
22. Compton, R. N., Carman, H. S., Desfrancois, C., Abdoul-Carime, H., Schermann, J. P., Hendricks, J., Lyapustina, S. A. and Bowen, K. H. *J. Chem. Phys.* 105 (1996) 3472.
23. Desfrancois, C., Abdoul-Carime, H., Khelifa, N., Schermann, J. P., Brenner, V. and Millié, P. *J. Chem. Phys.* 102 (1995) 4963.
24. Rossky, P. J. and Schnitker, J. S. *J. Phys. Chem.* 92 (1988) 4277.
25. Kondow, T. *J. Phys. Chem.* 91 (1987) 1307.
26. Markovich, G., Giniger, R., Levin, M. and Cheshnovsky, O. *J. Chem. Phys.* 95 (1991) 9416.
27. Knapp, M., Echt, O., Kreisler, D. and Recknagel, E. *J. Chem. Phys.* 85 (1986) 536; Misaizu, F., Kondow, T. and Kuchitsu, T. *Chem. Phys. Lett.* 178 (1991) 369; Campagnola, P. J., Posey, L. A. and Johnson, M. A. *J. Chem. Phys.* 95 (1991) 7998.
28. Desfrancois, C., Khelifa, N., Lisfi, A., Schermann, J. P., Eaton, J. G. and Bowen, K. H. *J. Chem. Phys.* 95 (1991) 760.
29. Jortner, J. *Z. Phys. D* 24 (1992) 247.
30. Barnett, R. N., Landman, U. and Nitzan, A. *J. Chem. Phys.* 91 (1989) 5567; Stampfli, P. *Phys. Rep.* 255 (1995) 1.

Received June 24, 1996.